Active Flow Control by Adaptive Blade Systems in Periodic Unsteady Flow Conditions

Steffen Hammer[1], Dat Tien Phan[2], Julija Peter[1], Tobias Werder[2], Robert Meyer[3], Robert Liebich[2] and Paul Uwe Thamsen[1],

[1] Technische Universität Berlin, Department of Fluid System Dynamics,
Strasse des 17. Juni 135, 10623 Berlin, Germany
steffen.hammer@fsd.tu-berlin.de, julija.peter@fsd.tu-berlin.de,
paul-uwe.thamsen@tu-berlin.de

[2] Technische Universität Berlin, Department of Engineering Design & Product Reliability,
Strasse des 17. Juni 135, 10623 Berlin, Germany
t.phan@tu-berlin.de, robert.liebich@tu-berlin.de

[3] DLR, German Aerospace Centre, D-10623 Berlin, Germany
robert.meyer@dlr.de

Abstract. A test stand to investigate the rotor-stator interaction of a compressor stage is presented. This water channel allows to investigate the influence of wake depressions and choking to a stator cascade. Furthermore, adaptive blade systems are presented to affect the operating of stator under periodic unsteady flow conditions. The piezoelectric actuators are one of these adaptive blade systems. These can adjust the profile, so that the stator is more efficient than without.

Keywords: adaptive blade systems, stator cascade, piezoelectric actuator

1 Introduction

Within the scope of the Collaborative Research Centre 1029, pulsating combustion contribute to a significant increase in the efficiency of a gas turbine. The pulsating combustion leads to periodic unsteady flow conditions in the compressor of the gas turbine. Due to the resulting periodic flow a flow angle increase in the compressor stage is induced, which results in additional losses by detached flow at the stator. Furthermore, the velocity deficit in the wake depressions of the rotor leads to an increase of the flow angle of the following stator. These two effects are superimposed in the case of the pulsating combustion. Figure 1 shows the corresponding velocity triangles.

As part of the Collaborative Research Center the rotor-stator interactions are to be influenced by means of adaptive blade systems. By this the working range of the compressor is stabilized and enhanced.

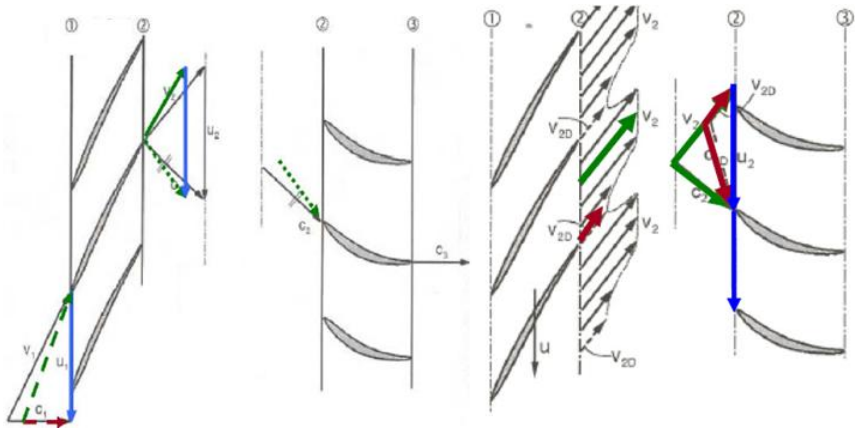

a) b)

Fig. 1. a) Effect of choke on inflow and outflow of a rotor and stator b) Effect of wake depression on the stator according to Bräunling [1]

2 Methods

For the active control of the angle of attack change four adaptive blade systems are studied. These blade systems adjust the stator blades, making them work as ideally as possible despite the misaligned flow.

The experimental investigations take place in a water flow channel at the Department of Fluid System Dynamics at the Technische Universität Berlin in a 2D measurement section.

Adaptive blade systems

Fig. 2 shows the four adaptive blade systems schematically. These are a blade with a movable leading edge as a further development of the adjustable blade, the blade with a Gurney flap and the blade with piezoelectric actuators. These can be used to influence the angle of attack changes.

By turning the adjustable blade (Fig. 2a), the critical angle of attack is prevented, and the blade works in a better range than the fixed blade. However, due to the adjustment of the entire blade the outflow angle is changed, so that the inlet flow of subsequent compressor stage is no longer ideal. To avoid this, a blade with a movable leading edge (Fig. 2b) is investigated. In this adaptive system, only the leading edge is adjusted, so that the exit flow is only slightly affected for the subsequent stage. The position of the leading edge flap and the flap angle are very important for the operation of the blade. Investigations by Jarius show that the flap position should be at 33% of the chord [8].

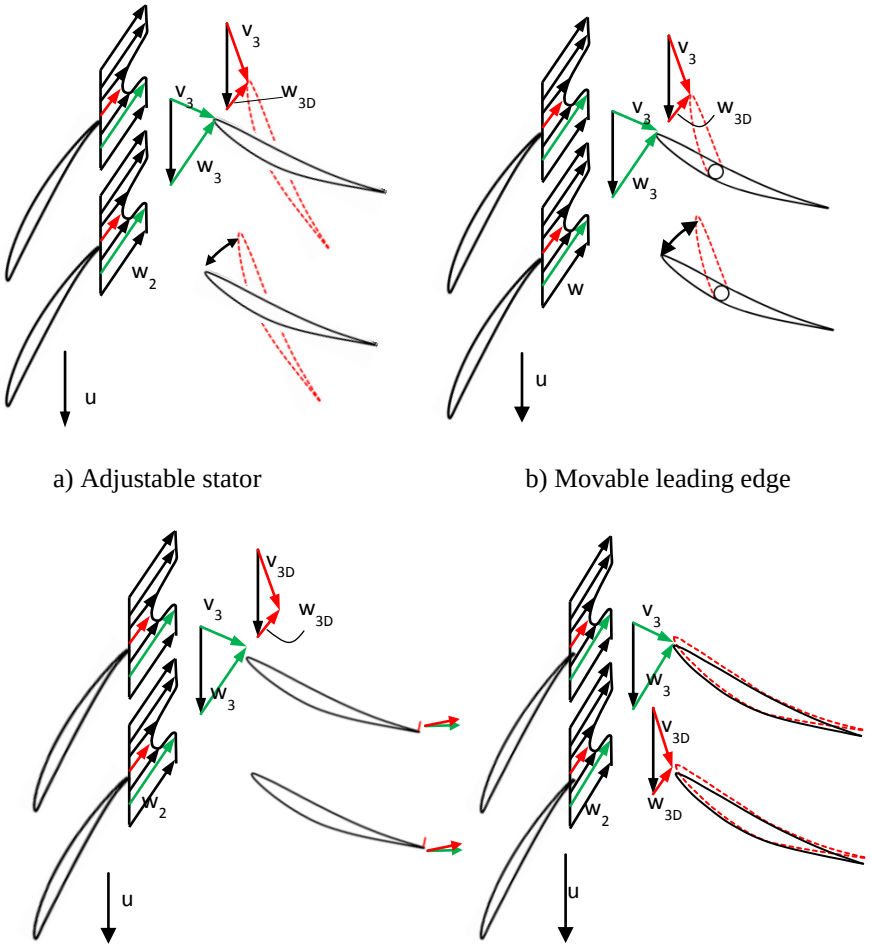

a) Adjustable stator b) Movable leading edge

c) Gurney flap d) Piezoelectric actuators

Fig. 2. Adaptive blade systems

As a third variant Gurney flaps attached to the blade trailing edge are investigated. Thus the curvature of the airfoil is increased. As a result, the stagnation point moves towards the Gurney flap. The stator also operates at misaligned flow.

The fourth adaptive blade system makes use of piezoelectric actuators, which are integrated into the blade profile. By applying voltage the piezoelectric actuator and the material are deformed. Thus the profile may be modified such that the misaligned flow is compensated for.

2.1 Test stand

At the Department of Fluid System Dynamics, a water flow channel is operated with nominal diameter of DN 400 (Fig. 3). The test stand is 10 m long, 1m wide and 4.5 m high. The capacity is about 7.7 m^3. The test rig is modular so that various investigations may be performed. The test rig is driven by a single-stage submersible pump (2) by Flowserve. The maximum volumetric flow is 1600 m^3/h at a head of 4.6 m. The flow is redirected by two bladed elbows (5). Afterwards the flow homogenization takes place with a 19-tube bundle straightener (6). Subsequently, a change in cross section from a round to the rectangular cross section is performed (7). In the test section, the stator cascade is integrated. After the test section the cross section changes from rectangular to round. The compensator (9) is used to compensate small length differences. The transition from the tank into the pipe section is fitted with butterfly valves to release only a portion of the water during assembly work on the measurement section.

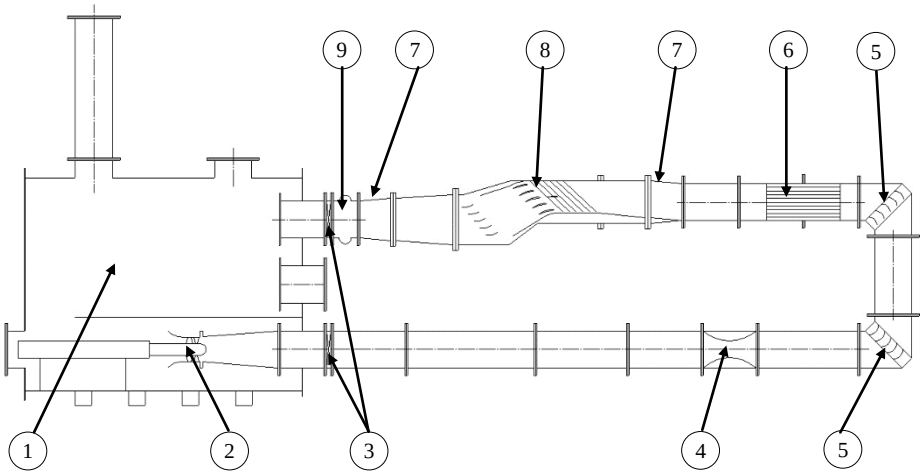

Fig. 3. Test stand at the Department of Fluid System Dynamics - 1 Tank 2 Submersible pump 3 Butterfly valves 4 Magnetic- inductive flow meter 5 Bladed elbow 6 19-tube tube bundle straightener 7 Change in cross section from round to rectangular 8 Measuring section 9 Compensator

Tank

The tank (Fig. 4) acts as a water reservoir having a volume of about 5.9 m^3. In the tank, the drive for the test stand is integrated. The single-stage submersible pump (1) can be extended by further stages if necessary. The motor is fixed by means a turnbuckle. At the height of the suction side of the pump wall pressure wells are integrated in the tank to measure the suction side pressure. Through the diffuser, the transi-

tion to the cross-section of DN 400 is realized. The partitions above the powertrain prevent a short circuit in the suction of the water and stiffen the tank additionally.

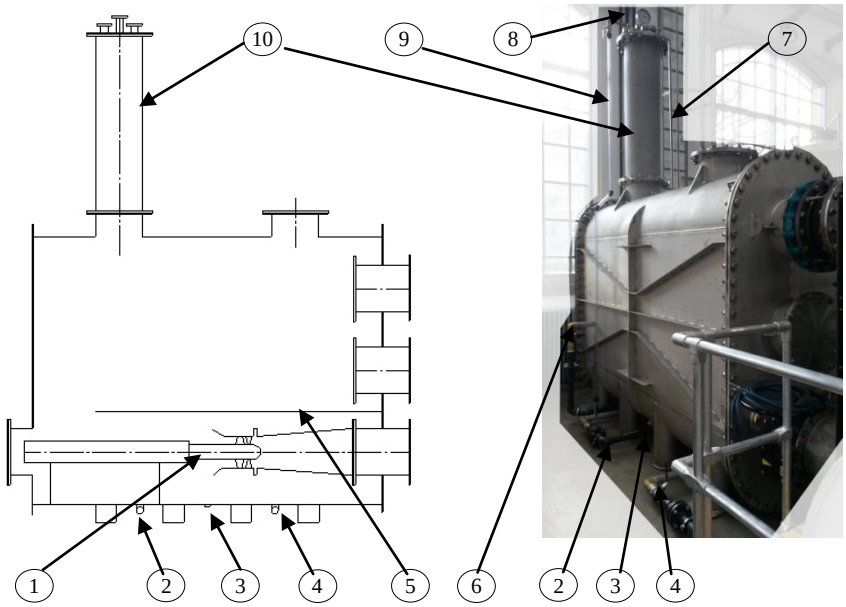

Fig. 4. Test tank - left schematically, right real 1 Submersible Pump 2 Cold water pipe 3 Pressure measurement 4 Filling 5 Partition plate 6 Warm water pipe 7 Pressure pipe 8 Dom cover 9 Water level indicator 10 Dom

The dom (10) is used to regulate the pressure in the test section. This is on the one hand influenced by the water column and on the other hand via a compressed air access (7), set in the dom cover. For measuring pressure in the tank a 10 bar pressure gauge is integrated in the dom cover. The built-in pressure relief valve prevents excessive pressure rise in the test stand. The filling and emptying (4) of the test stand is carried out via a DN 50 pipe at the front of the tank. The test stand is supplied from the water tanks of the experimental hall. To guarantee constant conditions concerning the Reynolds number the test stand is connected to the cooling system of the test field. Through the warm water pipe (6) the medium is removed and through the cold water pipe the cooled fluid is returned to the system. The stiffening rips on the tank surface prevent deformation of the tank at overpressure or negative pressure.

Deflection

The redirection is performed by means of two bladed elbows. These are preferred due to the small installation space compared to standard pipe elbows. The selection of an appropriate number and size of the blades was performed using of the simulation

software ANSYS. The calculations were performed as a 2D stationary calculation, incompressible and without heat equation in water. The volume flow is 1600 m^3/h. The results of the calculation are shown in Figure 5.

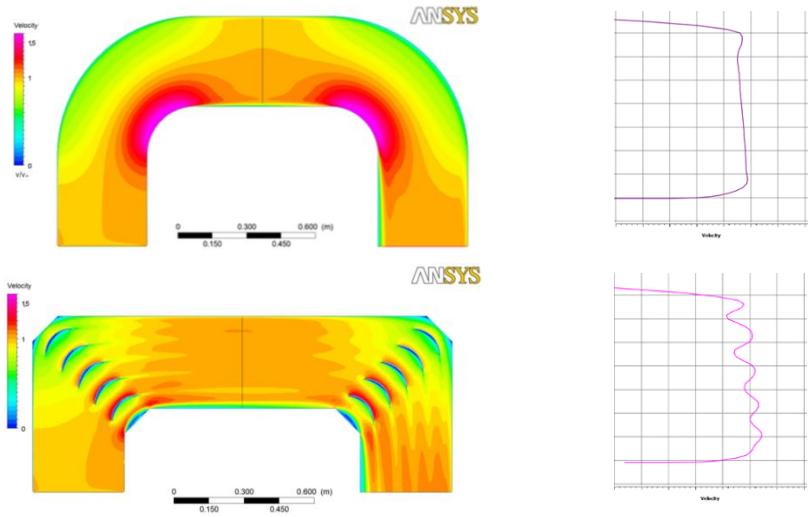

Fig. 5. Manifold – above standard elbow, below bladed manifold R=90, z=5

The illustration on the left shows the velocity distribution in the diversion passage. On the right side in Figure 5, the velocity profile at the outlet of the two manifolds can be seen. Obviously both velocity profiles are similar. However, the impact of the blades based on the wake depression is very clear. These are compensated by the subsequent 19-tube tube bundle straightener. The execution of the bladed elbow is shown in Figure 6.

Fig. 6. Bladed manifold

Measuring section

The test section allows the study of the important parameters for describing the operation of the stator by its modular design. The measuring section is designed as a rectangular duct having a cross section of 300 mm x 456 mm. The rectangular channel consists of frame racks. The back is closed with PVC panels. The remaining three sides are closed with acrylic glass plates to have optical access for laser optical measuring methods, such as Laser Doppler Velocimetry and Particle Image Velocimetry.

The test section is divided into four segments. In the first segment (3), an inlet guide vane is integrated to generate wake depression. To simulate the peripheral speed of the rotor, the inlet guide vane can be moved linearly along the grooves. It is possible to vary the axial distance between the stator and inlet guide vane in discrete steps.

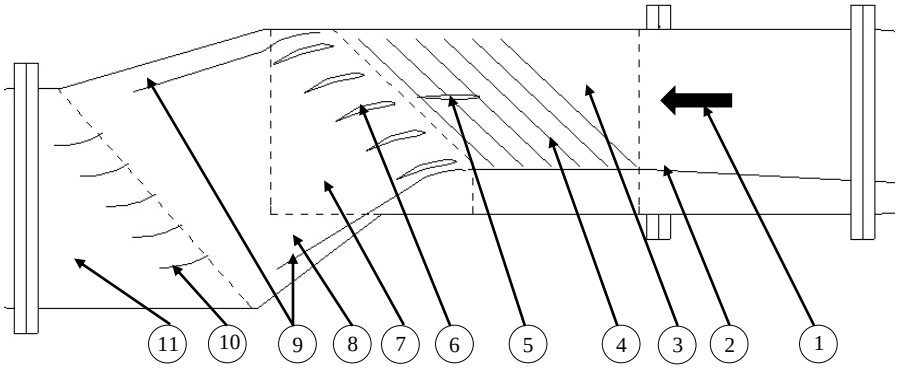

Fig. 7. Test stand - measuring section, dashed lines demonstrate segments boundary, solid lines demonstrate channel boundary 1 Flow direction 2 Variable channel wall to adjust the channel height 3 IGV plate 4 Guide vane structure Grooves for the displacement inlet guide vane 5 Inlet guide vane 6 Stator (measuring blade) 7 Stator grid 8 Caster 9 Channel wall to adjust the caster 10 Deflection plates 11 Deflector

The second segment (7) bears the stator cascade. It consists of five CDA profiles. This grid has been examined by Steinert et al. [5]. The blades are aligned by means of dowel pins. The stator inlet plane is parallel to the grooves of the guide-blade row. In order to vary the angle of attack at constant stagger angle of the stator, the channel walls of the stator blade row and inlet guide vane are replaced with the corresponding pin patterns and grooves. The resulting change in the channel height is compensated by the variable channel wall (2). The variable channel walls (9) in the wake of the stator are used to adjust the wake flow to the variable angle of attack.

The third and fourth segments, caster (8) and deflection (11), guide the flow parallel to the measuring section entrance. The deflection is realized with a sheet of metal. These segments are independent of the stator and inlet guide vane.

Investigation of morphing structures by piezoceramics

The purpose of our research is to suggest a new design concept of morphing structure for deformable and controllable leading and/or trailing edge of compressor blades by using piezoceramic materials. The first concept present a cross-section of a CDA (controlled diffusion airfoil) with a deformable leading edge. It is built in two parts. The trailing part is a solid body and the leading part a thin-walled structure and hollow. A piezo actuator is bonded to the inner side of the thin-walled structure. This thin-walled structure is mounted to the solid body part on the suction side. A gap on the pressure side between the thin-walled structure and the solid body part is closed by a thin membrane that covered the entire perimeter of the cross-section. The gap enables a higher deflection of the blade's leading edge.

In comparison to other concepts, this design is simpler, can even be produced as only one part and does not alter base geometry of the blade. The deformed leading part was made of the same material as the blade instead of composite or flexible materials [9 and 14] and its fabrication does not require a new production technology. The thin membrane was not used to supply PBP-actuators (post-buckled pre-compressed) [9] or to support airfoil shape [10]. But it was used to facilitate a smoothing and a continuity of the blade's shape and to protect electrical components against outside flow. The importance of the smooth continuous shape has been noted in several studies as an advantage over conventional flaps. The using piezo actuator is a DuraAct (piezoelectric patch transducer), which consists of piezoceramic plates instead of piezoceramic fibers of MFC. Its reliability has been rated to be better due to a new production technology. They can also be applied to curved surfaces or used for integration into structures. The piezo actuator bonded inside of the leading part does not interfere with the flow around the blade. This concept has a higher frequency and broader bandwidth for the actuation compared to the other concepts of actuated leading edge using conventional mechanical system [11, 12 and 13]. This allows the system to react in real time to high frequency choking or wake depression as a result of a pressure-increasing pulsating combustion, which is investigated within the scope of the Collaborative Research Center 1029.

Although the higher deflection can be achieved with this new concept, a small deformation of this flexible leading section before actuating can still occur due to a high flow pressure. The stiffness of this leading section can be varied by changing of the material type or the thickness of the thin-walled structure and the membrane to prevent this deformation as well as to fulfill more requirements having regard to flow conditions of the compressor blades.

3.1 Experimental investigation

One option for a modification of a blade is to place a thin-walled structure instead of a full blade at the leading or trailing part. Piezoelectric actuators excite oscillations in this structure and thus the blade inlet or outlet angle can be adapted according to a periodic flow change. In a first step a feasibility study of such a blade modification by using piezoelectric actuators was started. For the experimental setup a subsonic controlled diffusion airfoil (CDA) was chosen. The airfoil is representative of the rotor hub suction of an industrial axial flow compressor. The data of the airfoil and the cascade design is given in [4, 5 and 6]. The test rig is shown in Fig. 8.

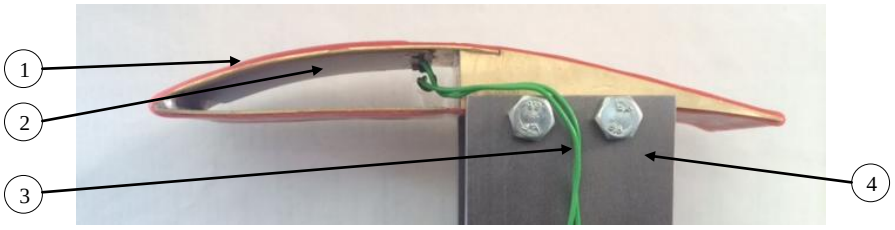

Fig. 8. Modified blade with an actuated leading part using piezoelectric actuators – 1 Elastomer membrane 2 Piezoelectric patch transducer 3 Supply cables 4 Clamping device

The thin-walled structure is made of the same material as the blade. It is 1 mm thick and about 70 mm long to match the chosen actuator. The actuator is attached inside this structure by using glue to secure the force transmission. The mounting of the thin-walled structure to the rest of the blade was also carried out on the suction side by using the adhesive or by screwing. A small gap occurs on the pressure side because there was no connection of the structure to the rest of the blade. Therefore a membrane is used to close this gap. Thereby, Elastosil M 4642 A/B from Wacker Chemie AG is used. Additionally this thin membrane protects electrical components against external influences. It smooths the blade's surface and increases the stiffness of the leading part. This membrane was glued on the blade's surface or cast around the blade by using a suitable casting mould.

In comparison to conventional mechanical control of the stagger angle known from gas turbines, the represented adjustable blades using piezoelectric actuators have a broader frequency range for the actuation. This allows the system to react to high frequency choking in real time. In addition, the piezoelectric patch transducer P876-DuraAct supplied by PI Ceramic needs less space than conventional piezoelectric stack actuators and can be applied evenly to a curved surface in particular.

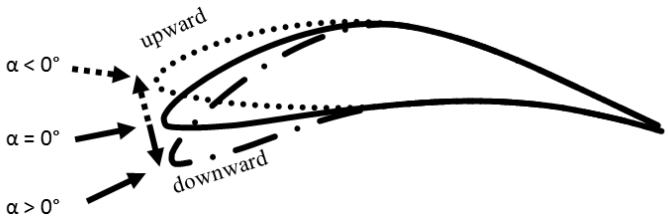

Fig. 9. Oscillation of leading part for periodically increasing and reducing flow inlet angle

During the first experimental investigations of the test rig the periodic deflections of the blade's leading edge were measured for different voltage levels from 50 V to 500 V peak-to-peak and an operating frequency of 78 Hz was applied to the piezoelectric actuators. This experimental feasibility study should show the necessary electrical power to reach the needed levels of deflection. The deflection of the leading edge which oscillates around its position of rest reached 7 mm peak-to-peak (see Fig. 9 and Fig. 10). This is equal to an oscillation about three degrees around the chord line. Thereby the actuator was supplied with the power of about 10 Watt.

As already mentioned, this experimental study should only show the potential to get the highest deflection of this actuated blade. Therefore the used operating frequency is very close to the first eigenfrequency of this structure. But operating in resonance could shorten the working life of the structure. For later works, the structure will be modified so that its eigenfrequencies are not close to the given frequency of the periodic choking so that the working life will not be affected strongly but a sufficient deflection will be reached.

Because the leading part of this actuated blade moves not only downwards but also upwards as described above, this blade system is ideally suited to adjust the flow inlet angle, which increases and reduces periodically (Fig. 9). However, in case the flow inlet angle only increases, then e.g. the stagger angle of the blade should be adjusted mechanically in advance or the leading part should be bent down in advance so that this leading part oscillates between the design flow inlet angle and the changed flow inlet angle as shown in Fig. 11. Another opportunity is a one-sided oscillating deflection to the position of rest. But such a one-sided oscillating deflection requires a complex instrumentation and control system. These development plans must be still investigated in more detail.

Furthermore, even a static deflection by applying a DC voltage is possible if necessary. However, these deflections are relatively small compared to the both-sided oscillating deflection (see Fig. 10).

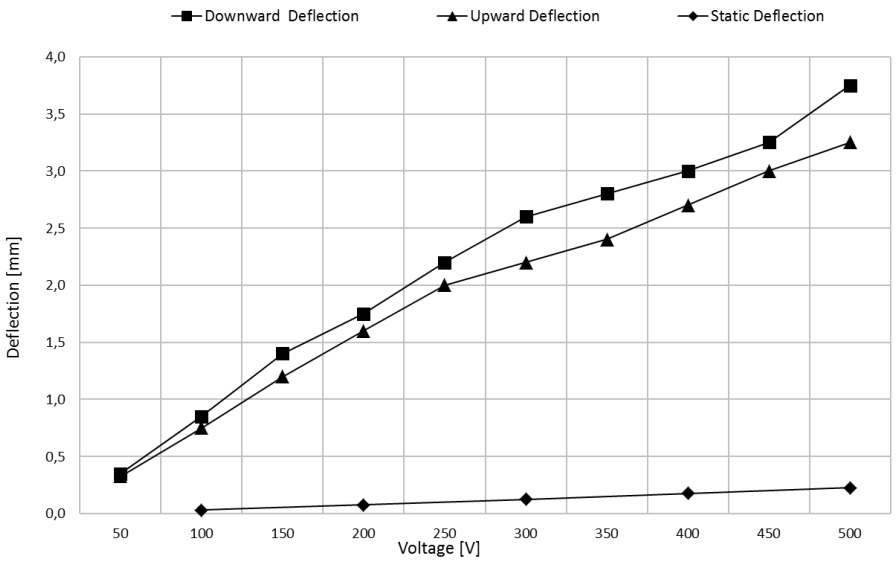

Fig. 10. Measurement data of deformed blade - Both-side oscillating deflection

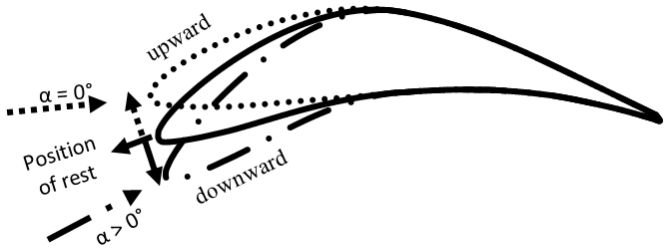

Fig. 11. Oscillation of leading part only for periodically increasing flow inlet angle

3.2 Numerical Investigations

In order to investigate the influence of an actuated blade on the flow in a first and rough examination, this blade is assumed as a single airfoil without consideration of the interference effects between blades. In order to compare the flow conditions of the datum and the actuated modified profile, first of all aerodynamic variables such as the pressure coefficient C_P, the lift coefficient C_L and the drag coefficient C_D were calculated using the XFOIL software at different angles of attack. These resemble different flow inlet angles caused by the wake depression or the periodic choking. The flow calculations were performed for water flow conditions as the first test will be per-

formed in a water channel. During the simulation of the circulation a Reynolds Number of $6.6 \cdot 10^5$ was chosen. The Mach number was selected smaller than 0.3 in order to guarantee an incompressible flow.

Furthermore, the FEM software ANSYS was used to investigate the structural system behaviour. ANSYS depicted a mechanical coupling between piezoelectric actuators and the blade-system consisting of a thin-walled structure and the rest of the blade. For this purpose, the effect of the piezoelectric patch transducer on the thin-walled structure was simulated in order to model its deformation without consideration of flow conditions. This simulation serves as the basis for a more detailed consideration of the coupling behaviour between the piezoelectric patches and a curved structure later.

After that, a deformed blade geometry was extracted from ANSYS and used to calculate aerodynamic variables in XFOIL in a static flow simulation. In order to investigate how the flow can be influenced by active adjustment, the pressure distribution around a CDA-profile was calculated additionally as shown in Fig. 12.

First numerical simulations were performed on the datum blade and the actuated blade. Figures 12a, 12b, 12d and 12f show the pressure distributions on the datum blade profile in case of four different angles of attack (0°, 1°, 3° and 5°). Figures 12c, 12e and 12g show the pressure distributions of the blade bent down by the piezoelectric actuators in case of the angle of attack being at 1°, 3° and 5° as shown in Fig. 11. The numerical results show the possibility to compensate the influence of an unsteady flow by adapting the blade according to the flow driven angle of attack. As shown in Fig. 12, the suction peaks at the leading edge of the datum blade which appear at high angles of attack can be avoided in part or completely by means of the deformed blades. In particular the leading edge stall in case of large angles of attack could be prevented [7] as shown in Fig. 12g.

Furthermore, the transition point on the suction side which moves towards the leading edge from 60% to 2% of the chord length, when the angle of attack increases from 0° to 5°. Obviously, this transition point does not move towards the leading edge due to the deformed blades (Fig. 12g). Thus a longer laminar boundary layer is guaranteed [2]. The friction losses can be reduced hereby (Fig. 14).

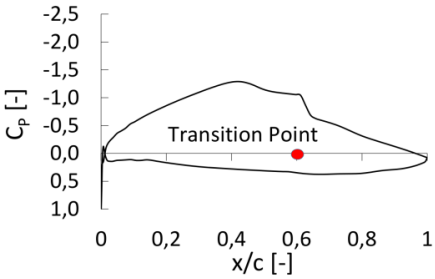

(a) Datum blade α=0°

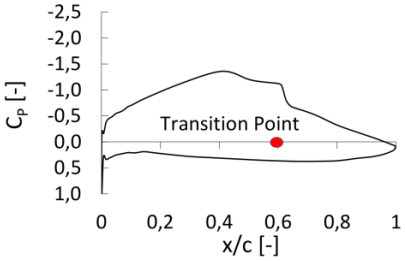

(b) Datum blade α=1°

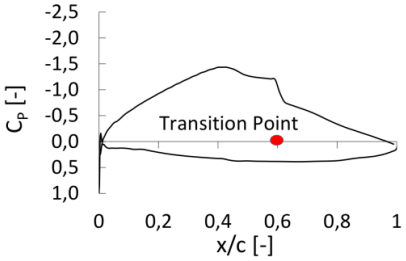

(c) 1° Deformed blade α=1°

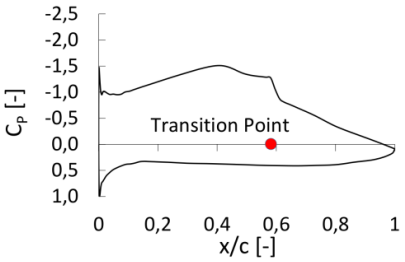

(d) Datum blade α=3°

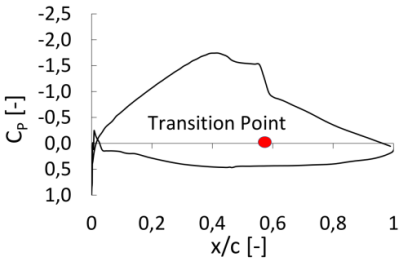

(e) 3° Deformed blade α=3°

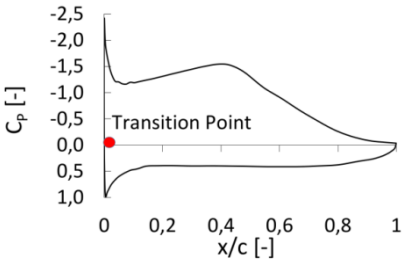

(f) Datum blade α=5°

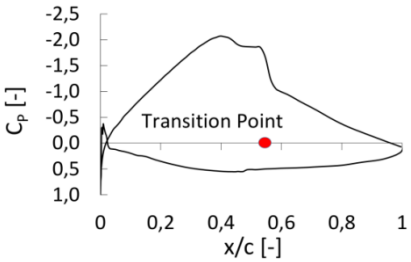

(g) 5° Deformed blade α=5°

Fig. 12. Pressure distribution around the blade profile

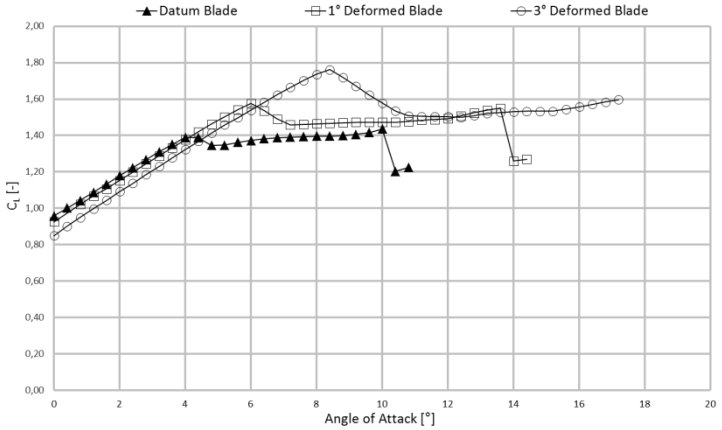

Fig. 13. XFOIL – Polar Diagram Lift coefficient

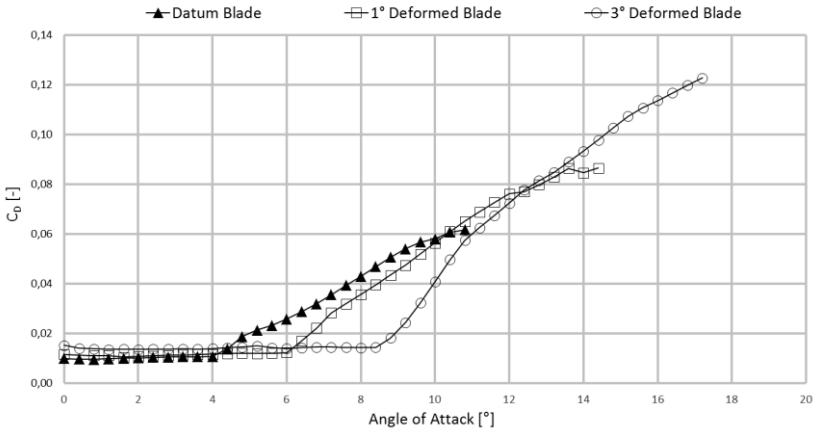

Fig. 14. XFOIL - Polar diagram drag Coefficient

The polar diagrams generated by XFOIL are shown in Fig. 13 and Fig. 14. The lift coefficient of the datum blade decreases abruptly at an angle of attack of 4°. From this angle on the drag coefficient also increases remarkably. The reason for this is that from this critical angle on a non-stable region appears and the transition point of the boundary layer of the suction surface moves upstream. Thereby the laminar separation bubble disappears and unsteady separation could occur (Fig. 12f). This critical angle can be increased by raising the radius of the nose or by changing the blade inlet angle.

In this work, the blade inlet angle was changed by bending up or bending down the leading part of the blade using actuators. Thereby the profile is adjusted to changing the flow angle.

Figures 13 and 14 show that deformed blades, in which the leading part bends down about 1° and 3°, have higher critical angles than the datum blade, respectively 6° and 8°. That means, the operating range is extended.

In addition, at low angles of attack the 1° and 3° deformed blades have slightly lower lift coefficients C_L and slightly higher drag coefficients C_D than the datum blade. This can be interpreted as result of the change of the blade shape caused by actuation (higher curvature). On the contrary, at higher angles of attack these coefficients are improved in comparison to the datum blade.

As already mentioned before, for calculating these aerodynamic variables using XFOIL, the blade was assumed as an infinite or endless aerofoil and is not influenced by the interference effects between blades. In order to examine the plausibility of these XFOIL results for a cascade application the MISES software was used. This software has also the basic functionalities as those of XFOIL but is able to analyse the flow through cascades in turbo-machinery. Hence influences caused by the finite blade and the interference effects between blades can be considered.

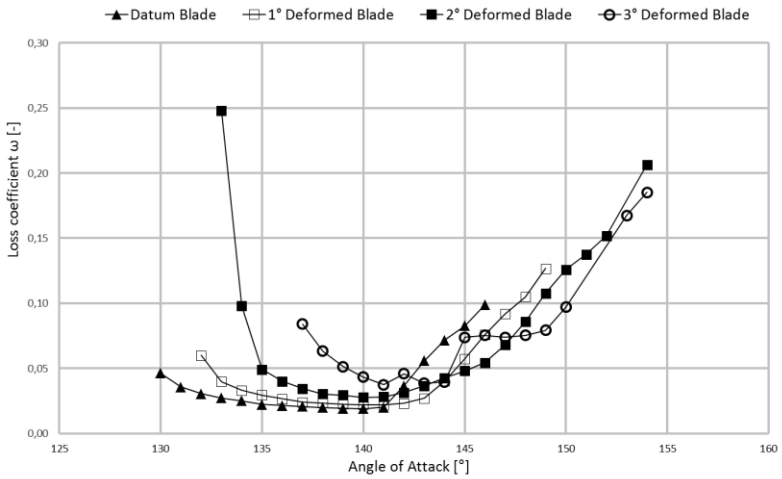

Fig. 15. MISES - Polar diagram

Figure 15 shows the loss coefficient as function of flow inlet angle with reference to circumferential direction. It can be seen that the loss coefficient of the datum blade rises for a negative and a high positive incidence in comparison to the design point at a flow inlet angle of 137°. For a positive incidence, the loss coefficient declines slightly and then from an angle of 141° onwards the loss coefficient rises remarkably. The flow inlet angle of 141° corresponds to the design point with an angle of incidence of 4°. That is comparable to the polar diagram generated by XFOIL (Fig. 13,

14), in which the lift and drag coefficient also increase remarkably at the angle of attack of 4°.

Furthermore, the operating range will also be extended about two degrees in case the 1° deformed blade is used. Thereby the loss coefficient of this deformed blade begins to increase remarkably from the flow inlet angle of 143° corresponding with an angle of incidence of 6°. These simulation results are comparable with the measurement results published in [5]. With a 3° deformed blade the operating range will be extended about three degrees only, instead of four degrees as the result generated by XFOIL. In addition, the loss coefficient of this 3° deformed blade is much higher than the one from the datum blade, the 1° and 2° deformed blade. Therefore an application of actuated blades leading to deformation higher than the 3° deformed blade does not bring a benefit. The blade shape would change strongly so that the loss coefficient of this deformed blade is very high all over. That means, only small deformed blade due to actuation could bring about good effects.

Summary

A test stand was developed, which allows the investigation of angle of attack changes to a stator cascade. In the 2D measurement section rotor-stator-interaction and active flow control by adaptive blade systems will be studied.

The first experimental and numerical investigations showed a principal feasibility of using piezoelectric actuators for adaptive blade control in case of unsteady flow with periodic choke in particular. The behaviour in actual operation will be investigated in the presented water flow channel. To this aim, blade-systems have to be designed broader and adjusted so that these modified blades are even functional in liquid media. For this broader blade a design with several actuators put side by side can be used as shown in the preliminary investigations.

In addition, modified blade-systems will be improved in order to validate the results of the modelling better and to get higher deflection having regard to flow conditions. In the later project phase, an instrumentation and control system will be developed so that the actuated blade can react in real time on the actual flow conditions. Hereby the pressure distribution is the variable to control and the change of blade inlet angle is the actuating variable. Additionally unsteady flow simulations will be carried out to supplement the experimental investigations.

Acknowledgement

The presented results were produced within the project “CRC 1029 - TurbIn” funded by the German Research Foundation (DFG). Furthermore, the authors would like to thank their project partners for the great collaboration.

References

1. Bräunling, W.: Flugzeugtriebwerke. Springer-Verlag, 2nd edition 2004
2. Dubs, F.: Aerodynamik der reinen Unterschallströmung. Birkhäuser, 4th edition 1979
3. The Institute of Electrical and Electronics Engineers: IEEE Standard on Piezoelectricity. In: ANSI/IEEE Std 176-1987
4. Steinert, W., Eisenberg, B., Starken, H.: Design and Testing of a Controlled Diffusion Airfoil Cascade for Industrial Axial Flow Compressor Application. In: ASME. Volume 113. (1991) 583-590
5. Steinert, W., Starken, H.: Off-Design Transition and Separation Behavior of a CDA Cascade. In: ASME. Volume 118. (1996) 204-210
6. Schreiber, H.A., Steinert, W., Kuesters, B.: Effects of Reynolds Numbers and Free-Stream Turbulence on Boundary Layer Transition in a Compressor Cascade. In: ASME. Volume 124. (2002) 1-9
7. Schlichting, H., Truckenbrodt, E.: Aerodynamik des Flugzeuges. Erster Band: Grundlagen aus der Strömungsmechanik. Springer-Verlag, 3rd edition 2001
8. Jarius, Mark: Untersuchung einer Axialgitterschaufel mit Höchstumlenkung durch Struktur- und niederfrequente Wölbungsvariation. PhD thesis 2000
9. Vos, R, Barrett, R., Krakers, L. and van Tooren, M.: Post-Buckled Precompressed (PBP) piezoelectric actuators for UAV flight control. In: SPIE. Volume 6173. (2006) DOI: 10.1117/12.658695
10. Maucher, C.K., Grohmann, B.A., Jänker, P., Altmikus, A., Jensen, F. and Baier, H.: Actuator Design for the Active Trailing Edge of a Helicopter Rotor Blade. In: Proceedings of the 33rd European Rotorcraft Forum, Kazan, Russia. 923-961
11. Chandrasekhara, M.S., Martin, P.B. and Tung, C.: Compressible Dynamic Stall Control Using a Variable Droop Leading Edge Airfoil. In: Journal of Aircraft. Volume 41. No. 4. (2004) 862-869
12. Kintscher, M., Wiedemann, M., Monner, H.P., Heintze, O. and Kühn, T.: Design of a smart leading edge device for low speed wind tunnel tests in the European project SADE. In: International Journal of Structural Integrity. Volume 2. No. 4. (2011) 383-405 DOI: 10.1108/17579861111183911
13. Tomassetti, G., Ameduri, S. and Carozza, A.: Innovative streamline-flow preserving actuation strategies for wing airfoil nose. In: International Journal of Structural Integrity. Volume 2. No. 4. (2011) 437-457 DOI: 10.1108/17579861111183939
14. Bilgen, O., Butt, L. M., Day, S. R., Sossi C. A., Weaver, J. P., Wolek, A., Mason, W. H., Inman, D. J.: A novel unmanned aircraft with solid-state control surface: Analysis and flight demonstration. In: Journal of Intelligent Material Systems and Structures. Volume 24. No. 2. (2012) 147-167